IEEE Access
Multidisciplinary | Rapid Review | Open Access Journal

Date of publication xxxx 00, 0000, date of current version xxxx 00, 0000.

Digital Object Identifier 10.1109/ACCESS.2017.Doi Number

Analysis and Experimental Verification of the Peaking Capacitor's Flashover Process in an EMP Simulator

Yi Wang, Zhiqiang Chen, Wei Jia, Wei Wu, Le Cheng, Linshen Xie, Gang Wu, AND Kaisheng Mei

State Key Laboratory of Intense Pulsed Radiation Simulation and Effect (Northwest Institute of Nuclear Technology), Xi'an, 710024 China

Corresponding author: Wei Jia (host819@ 126.com).

This work was supported by the Fund of State Key Laboratory of Intense Pulsed Radiation Simulation and Effect under Grant C088220502.

ABSTRACT The flashover process of the peaking capacitor in the electromagnetic pulse (EMP) simulator is studied based on theoretical analyses and experimental verification in this paper. There are deeper and denser ablation spots on the film surface near the inner core of the destroyed peaking capacitor, while the damage of the outer film is relatively slight, which indicates that the flashover current along the inner film is larger. Besides, the circuit simulation analyses show that the earlier the flashover occurs on the film of the peaking capacitor, the smaller the flashover current. The electric field on the non-conical surface of the capacitor is mainly occupied with normal component. Differently, for the conical surface, the electric field on the outer layer is dominated by the normal component and the parallel component is the main part on the inner layer. It is considered that the flashover on the conical surface originates from outer layers and develops gradually to the inner until the flashover penetrates through all layers. Furthermore, the images of flashover show that the flashover firstly occurs on the outermost layers and develops to the inner layers with the increase of the voltage. For such special structure of the peaking capacitor, the parallel component of electric field is more likely to facilitate the flashover under nanosecond pulse. These results may exhibit specific reference implication in the design of insulation for the peaking capacitor used in EMP simulator.

INDEX TERMS EMP simulator, flashover, nanosecond pulse, peaking capacitor

I. INTRODUCTION

The electromagnetic pulse (EMP) simulator is widely applied to detect the anti-electromagnetic pulse capability of the electronic system under strong electromagnetic radiation environment [1]-[3]. In order to meet the requirements for the waveform with faster rise time and narrower full-width at half-maximum (FWHM) of the EMP pulse for some large EMP simulators under MV voltage, the one-stage or two-stage pulse compression technique are usually adopted in the EMP simulators [4], [5].

In the scheme of the one-stage or two-stage pulse compression, the peaking capacitor is one of the important components for the simulator to compress the pulse in the last stage circuit, and in conjunction with the output switch, the pulse with steep rise time is fed into the antenna. In order to avoid too large equivalent inductance of the peaking capacitor deteriorating the rise time of the output waveform, the capacitor is mostly designed with coaxial structure in some large EMP simulators [6]-[8]. For the aim of reducing the inductance of the last stage of pulse compression circuit and shortening the discontinuous sections of the conical radiation antenna, the peaking capacitor is placed at the top of the conical antenna, and the cone angle of the peaking capacitor is designed to be the same as the antenna [9]. For the requirement of low inductance, the structure of the peaking capacitor is more compact. The distance between the high voltage electrode and ground electrode is relatively shorter. Thus, the safety margin of insulation for the peaking capacitor is comparatively smaller than other parts of the simulator. The peaking capacitor is coaxially formed with a laminated structure which consists of alternative multiple coaxial electrodes and polypropylene film layers. The film layers are soft and extend a certain distance than the edge of the electrodes, which may cause the connection between the neighboring layers of the film. Furthermore, it tends to occur flashover on the surface of the film. The insulation failure is easily caused by surface flashover under nanosecond Pulse with high voltage [10], [11].

The flashover under nanosecond pulse would experience three typical phases: initial phase, developing phase, and extinguishing phase, and the surface charge would affect the flashover performance of dielectrics in vacuum [12], [13]. The flashover voltage rose linearly at first and then reached its maximum when gas pressure increased in SF_6 under the nanosecond pulse, and the development of flashover could be divided into several periods [14]. Q. Xie *et al*. also proposed that the flashover voltage increased with the pressure of the SF_6 under Microsecond-pulse, and the material surface sequentially evolved into different zones during the aging process [15]. J.T. Krile *et al*. revealed a material dependence on the discharge path of the surface flashover along dielectric insulators in SF_6 environment [16]. The electric field also has an important influence on the surface flashover of dielectric insulators [17], [18].

For the Polypropylene Film, the surface charges that accumulate on polypropylene (PP) film can induce electrical field distortion and surface flashover [19], [20]. Z. Chen *et al*. has found that the breakdown of a thin polypropylene film is mainly determined by the electrical field but not the voltage-time cumulative effect [21]. The flashover voltage of the PP film increases with the SF_6 pressure linearly in low-pressure regions, and the growth of flashover voltage gradually slows down and approaches a saturation value in high-pressure regions [22]. The normal field component would increase the flashover voltage in a low gas pressure region in SF_6 [23]. Although much research about the characteristics of flashover for the dielectric under nanosecond pulse has been presented, the flashover and insulation failure process for such conical and coaxial peaking capacitor with the laminated structure has been no more reports before.

In this paper, the characteristics of the flashover trace on the different film layers of the peaking capacitor of insulation failure are summarized, and the flashover process of the peaking capacitor and the influence of electric field on the flashover surface of the film layers are analyzed based on the simulation results of circuit and electric field. Finally, these analyses are verified by obtaining the images of the flashover discharge on the conical surface of the peaking capacitor under different voltage grades.

II. THE FEATURES OF FLASHOVER TRACE ON THE PEAKING CAPACITOR

The cross section of the coaxial peaking capacitor is shown in Fig. 1. After winding several layers of polypropylene (PP) film on the inner core electrode, the metal cylindrical ring electrode is used to tighten the film, then each film layer is arranged with a metal cylindrical ring electrode. The film layers stretch a certain distance than the edge of cylindrical electrodes to ensure the insulation performance on the film surface. Each film layer and two electrodes on both sides can form a small single coaxial capacitor, and the peaking capacitor in this paper can be considered to be comprised of 18 small single coaxial film capacitors in series with the equal capacitance. In order to guarantee the continuous natural impendence throughout the whole antenna, the outer contour of the electrodes on the conical surface of the peaking capacitor (Side A in Fig. 1) is designed with the same cone angle as the conical radiation antenna, while the outer contour of the electrodes on the non-conical surface (Side B in Fig. 1) is roughly perpendicular to the axis.

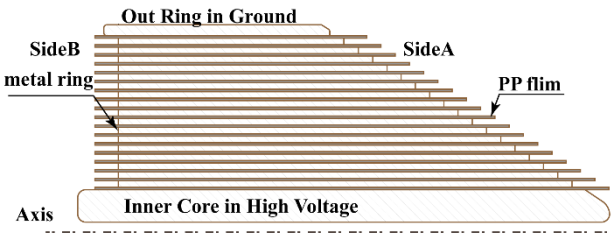

FIGURE 1. The cross section view of the peaking capacitor.

In an EMP simulator, the peaking capacitor is insulated by a high pressure SF_6 gaseous atmosphere because it is required to withstand the nanosecond pulse with a voltage of up to 2.5 MV. The structure of the peaking capacitor is very compact, and the designed margin of insulation for the capacitor is small. The surface flashover on the film is very easy to occur under the high voltage nanosecond pulse. The flashover trace on the surface of different layers after the insulation failure of the peaking capacitor is shown in Fig. 2. It can be seen that the flashover traces of the peaking capacitor are mainly concentrated on the conical surface in Side A. The conical surface is covered with some carbonized channels and ablative spots, which indicates that there is a serious flashover phenomenon on the conical surface before the insulation failure of the peaking capacitor.

FIGURE 2. Flashover traces on the conical surface of the peaking capacitor.

Fig. 3 shows the different film layers with the flashover traces on the conical surface in Side A of the disassembled damaged capacitor. It illustrates that the flashover traces on each layer behave different characteristics. There are two main types of the flashover channel. Fig.4 (a) shows that the flashover channel between the adjacent metal ring electrodes stretched from the upper electrode along the surface of the film to the lower electrode. The flashover channel shown in

Fig. 4 (b) extends from the edge of the upper film, and then develops towards to the lower layer and converges with the lower channel.

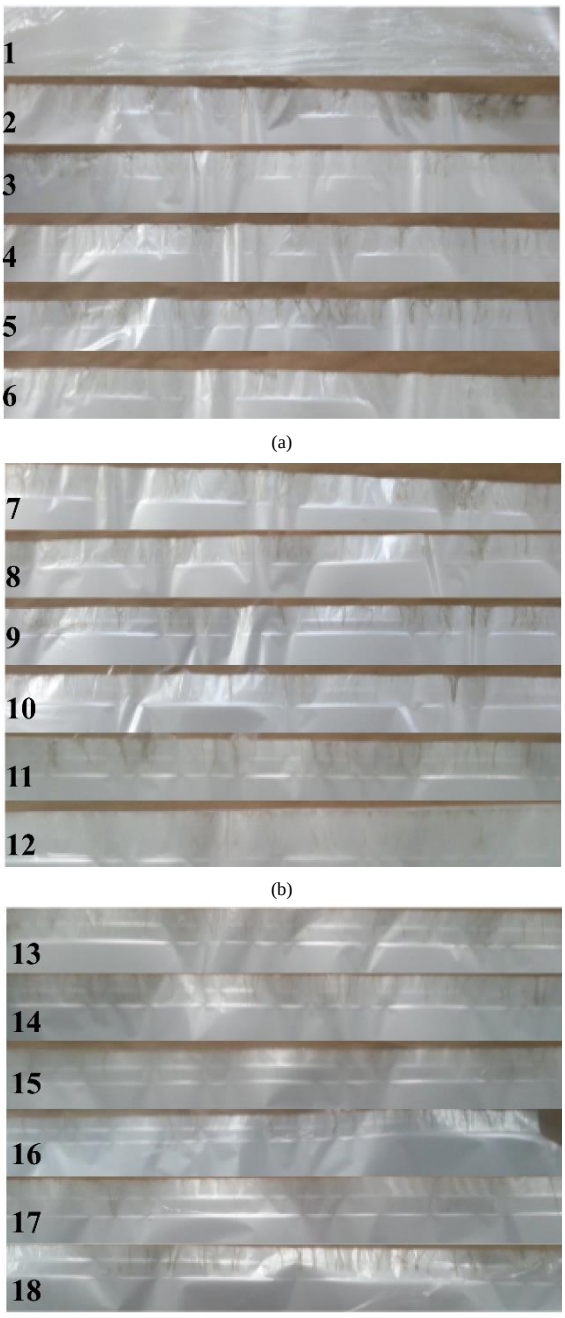

FIGURE 3. Flashover traces on the film surface of different layers. (a) Layer1-6. (b) Layer7-12. (c) Layer13-18.

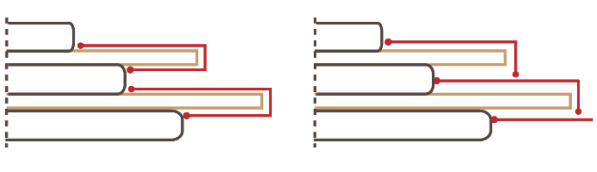

FIGURE 4. Two types of the flashover channel. (a) channel between both side. (b) channel jumping from upper layer to lower layer.

The film layer near the inner core of the peaking capacitor is marked as Layer 1, and the rest layer orders increase from inner to outer in turn. According to the flashover traces on each film layer of the peaking capacitor after insulation failure, the features of the flashover channels on the surface of the capacitor can be analyzed as follows.

1) On the non-conical surface in Side B, the flashover channels appear only on the Layer 1, while there is no flashover channel on the other layers, which might be correlated to the film clinging to the inner core electrode on the Layer 1 in Side B, resulting in the reduction of the insulation distance of the Layer 1.
2) On the conical surface in Side A, the Layer 2 is most severely damaged, and there are flashover traces on the upper and lower sides of the film layer, forming the channel as the type shown in Fig.4 (a). This phenomenon indicates that the surface flashover current of Layer 2 of the film is greater than other layers.
3) On the conical surface in Side A, the damage from Layer 3 to 7 is a little more severe than Layer 8 to 18. Overall, the damage from the outer layer to the inner layer is more serious.

III. CIRCUIT AND ELECTRIC FIELD SIMULATIONS

A. CIRCUIT SIMULATION

The voltage and current parameters in the equivalent circuit of EMP simulator would be changed due to the surface flashover on the film of the peaking capacitor, which can be analyzed by the circuit simulation. The two stages of pulse compression of the EMP simulator is shown in Fig. 5 (a). Firstly, in the first stage circuit of the pulse compression, after the erection of Marx generator (primary pulse source), the capacitor C_s (intermediate capacitor) is charged. When C_s reaches the specified voltage roughly equal to that of the Marx open-circuit output voltage, the intermediate switch S_1 closes rapidly and discharges into the peaking capacitor C_p. Similarly, when the voltage of the peaking capacitor is up to the same as the maximum charging voltage of the intermediate capacitor, the output switch S_2 is switched on and the antenna is discharged quickly by the peaking capacitor C_p. Then, the EMP pulse is radiated by the antenna.

As mentioned, the peaking capacitor can be equivalent to consist of 18 small single coaxial film capacitors in series. As shown in Fig. 5 (b), each coaxial capacitor can be considered to a small capacitor and a parallel circuit of the equivalent flashover branch when the flashover occurs on the film layer. The equivalent inductance and resistance of flashover channel can be calculated approximately according to the formula about the spark channel [2].

$$L \approx 14d \tag{1}$$

$$R \approx \frac{2}{V_m}\sqrt{\frac{pd^2}{a}}\sqrt[4]{\frac{L\times 10^{-9}}{C^3}} \tag{2}$$

where L is the equivalent inductance of the flashover channel (nH), d is the length of the spark channel (cm), R is the

equivalent resistance of the flashover channel (Ω), V_m is the voltage on the single small coaxial capacitor(V), C is the capacitance of the single small coaxial capacitor (F), p is the press of the gas (atm), a is a gas-related experimental constant, a ≈ 0.8~1.0 atm/(s • V2). The values of these parameters are d ≈ 0.7~0.8 cm, V_m ≈ 135 kV, C ≈ 2.52 nF, p ≈ 6 atm, a = 0.8, hence, L ≈ 9.8 ~11.2 nH, R ≈ 0.44~0.52 Ω.

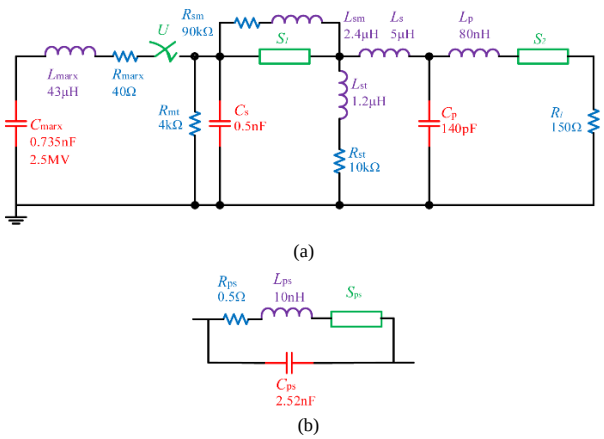

FIGURE 5. The circuit simulation model. (a) the equivalent circuit of an EMP simulator. (b) the flashover branch.

The flashover branch consists of a self-breakdown switch S_{ps}, an equivalent resistor and an inductor in series. The equivalent resistance and inductance of the flashover branch can be set to 0.5 Ω and 10 nH respectively. The breakdown voltage of the self-breakdown switch S_{ps} can be used to indicate the flashover voltage of the film layer. The flashover moment of the film can be adjusted by changing the breakdown voltage of the self-breakdown switch, and the earlier the flashover occurs, the lower the flashover voltage. According to this simulation model, both the influence of flashover on one film layer to other layers and the influence to the output impulse can be investigated. The influence of different flashover time to the flashover current on the film layers can also be analyzed.

It is assumed that the flashover would firstly occur on the Layer 1, and the influence on the other layer small coaxial film capacitors can be analyzed. (Due to the capacitance of each layer is designed to be equal, the influence on the single coaxial capacitor of the Layer 2 can be taken as an example to be illustrated). The output voltage of Marx can be set to 2.5 MV in this model, and the voltage loaded in the peaking capacitor is about 2.44 MV when the output switch is closed, and the voltage of each small single coaxial capacitor is about withstand 135.7 kV. The series of self-breakdown switches wound not be closed when the voltage of each small single coaxial capacitor is a little larger than 135.7 kV. The threshold breakdown voltage of self-breakdown switch can be considered as the flashover voltage of the small single coaxial film capacitor. When the voltage of each small single coaxial capacitor is smaller than the threshold voltage of self-breakdown switch, there is no flashover on the single coaxial film capacitor. The flashover voltage of the first small single coaxial film capacitor could be set to 30 kV,60 kV,90 kV,120 kV,135 kV,150 kV respectively, which is also corresponding to the different flashover time, and there is no flashover on the film under the threshold voltage of 150 kV.

Fig. 6 shows the voltage waveforms of the second single coaxial film capacitor when the flashover arises on the first single coaxial capacitor under different voltages. As shown in Fig. 6, compared with the normal state under 150 kV, the relative variation of the rise time is about 4% and the relative variation of the amplitude is 5% under 30 kV. For the flashover voltage of 135 kV, the relative variation of the rise time is 0.3% and the relative variation of the amplitude is 0.4%. When the flashover voltage of the single capacitor on the Layer 1 is smaller, namely the flashover occurs at the earlier time, the relative change of pulse applied on Layer 2 is relatively obvious compared with the normal state. The relative variation is smaller when the flashover voltage approximates to the withstand voltage the single coaxial film capacitor, i.e. the flashover occurs during the latter period. It shows that the flashover on one film layer would have a great influence on the parameters of voltage waveform on the other layer coaxial capacitors only when the flashover voltage is low.

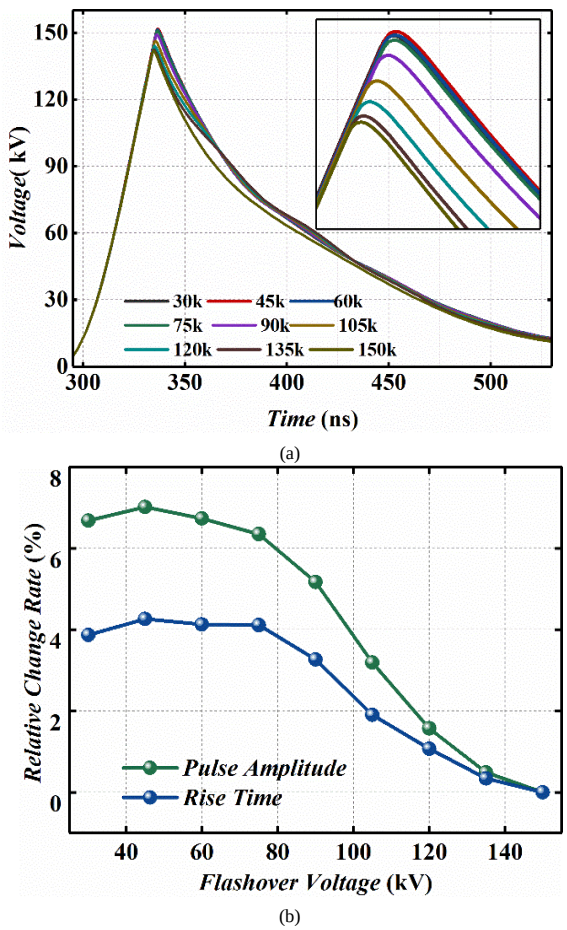

FIGURE 6. Influence of flashover voltage of one capacitor on another coaxial capacitor. (a) voltage waveform. (b) the relative variation under different flashover voltage.

Fig. 7 illustrates the flashover current waveform under the different flashover voltage on the Layer 1. It demonstrates that the positive peak value of the flashover current would gradually rise as the flashover voltage increasing, which is caused by the short circuit discharge of the single small coaxial film capacitor. As the flashover voltage increases on one layer, there is more energy stored in the single coaxial film capacitor and the flashover current increases as well. Moreover, the damage on the film becomes more serious. Therefore, the damage on the surface of the film would be more severe with a higher flashover voltage. In other words, when the flashover occurs later, more obvious flashover traces would be left on the surface.

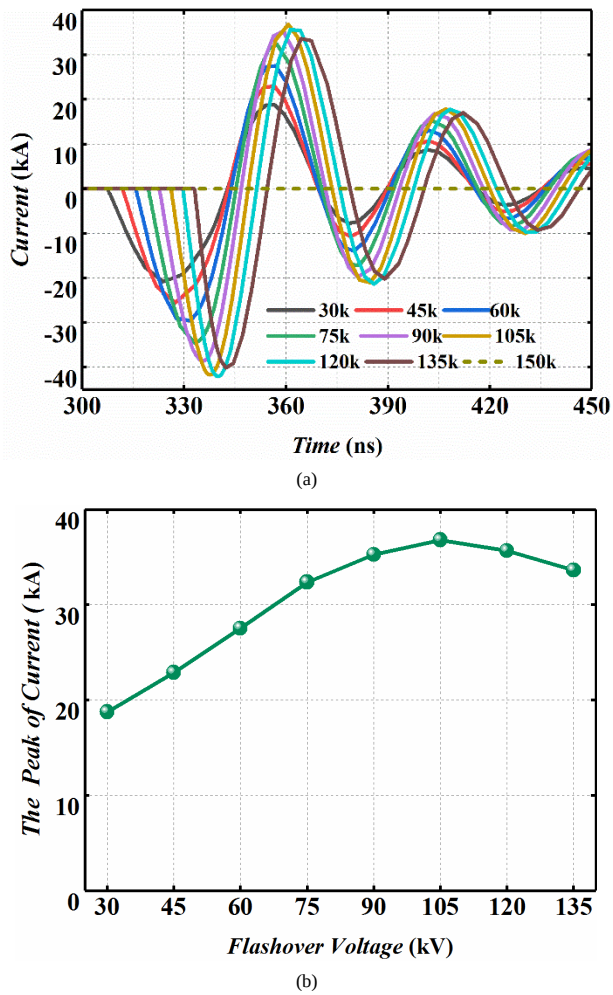

FIGURE 7. Influence of the flashover time on the flashover current of coaxil capacitor. (a) current waveform. (b) the positive peak value of flashover current.

The insulation failure of the peaking capacitor would happen as the flashover appeared on multiple layers of the dielectric film simultaneously. The influence of the number of the flashover layers on the output pulse voltage loaded on the antenna is shown in Fig. 8, where the flashover voltage of each small single coaxial film capacitor with flashover is set to 105 kV, and the threshold voltage of self-breakdown switch on the other small single coaxial film capacitor without flashover is set to 200 kV. The result shows that if the number of layers appearing the flashover is less than 3, compared with the normal condition without the flashover, the relative variation of the rise time and the amplitude is acceptable. There is the more obvious oscillation on the waveform when the number of flashover layers is 4. However, if the number of film layers is 5 or more for the parameters set in this paper, the voltage applied on the other small coaxial capacitor would exceed the threshold value of the flashover voltage and the flashover would bestrew on the whole peaking capacitor. The waveform of the output pulse voltage can't meet the specific requirements. It indicates that the distortion of the output pulse voltage will be more serious as the number of the flashover layer increases. If there is a certain number of film layers with flashover, the insulation failure of the peaking capacitor will be caused.

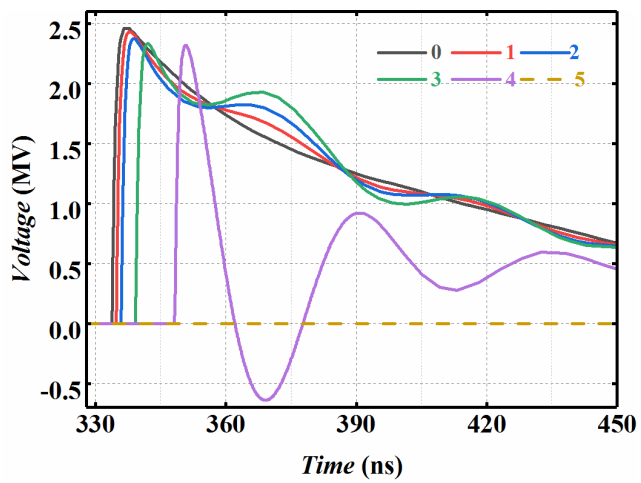

FIGURE 8. Comparison of output voltage waveform on the antenna under different number of the layers with flashover.

B. ELECTRIC FIELD SIMULATION

It is well known that the electric field on the surface of solid dielectric has a very important influence on the flashover process. The characteristics of flashover on the film surface can be studied by the distribution of electric field on the peaking capacitor. The inner core electrode of the peaking capacitor is loaded with the voltage of 2.5 MV, and the outer ring is grounded.

Fig. 9 (a) and (b) demonstrate the distribution of electric field on the upper and lower surface of all the layers in Side A. The X coordinate indicates the length of the outstretched part of each layer along axial direction. The curve of each layer begins from the edge of the film, and ends at the outer edge of the electrode. The electric field strength at the characteristic points (0 mm, 8 mm,16 mm and 24 mm) away from the outer edge of each layer film are chosen to compare the electric field strength on the different layers. As shown in Fig.9 (a) and (b), in Side A, the electric field on the surface of each layer changes with the similar trend along axial direction. The electric field strength on the film surface at the same position (such as the point at 8 mm and 16mm) away

from the outer edge of each layer almost decreases from inner layers to outer layers. However, the electric field strength near the triple point (24 mm) of each layer is nearly the same as each other.

Fig. 9 (c) and (d) show the distribution of electric field on the upper and lower surface of each layer on the non-conical surface in Side B. The insulation length of each layer is approximately equal on the non-conical surface, and the insulation distance in the Side B between high voltage electrode and the ground electrode is smaller than the Side A. Therefore, for the same position, the electric field in the Side B is slightly larger than the Side A. In the Side B, the electric field on the film surface at the same position of each layer is almost the same, and the field near the triple point (16 mm) of each layer is nearly the same as each other. Either in Side A or B, the field at the triple point of each layer is approximately equal, however, the characteristics of flashover traces on each layer is different, which shows that the sudden distortion of the field near the triple point is not the main reason for the surface flashover and partial discharge on the film surface.

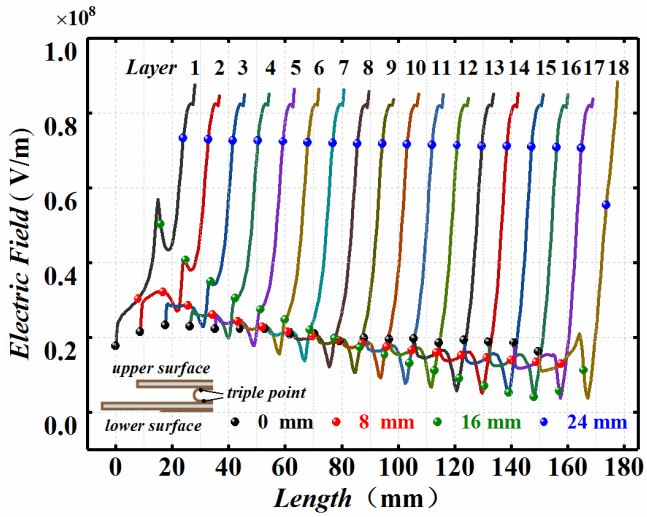

(a)

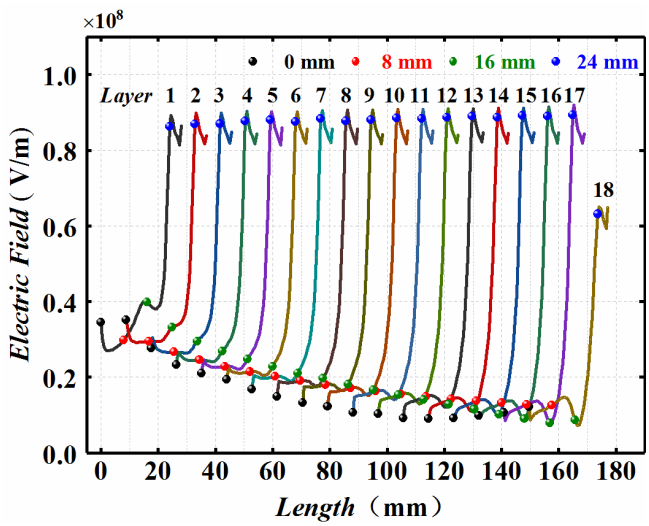

(b)

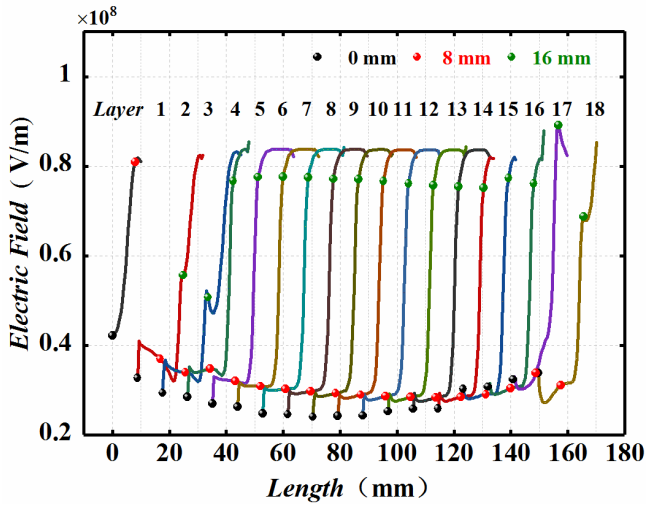

(c)

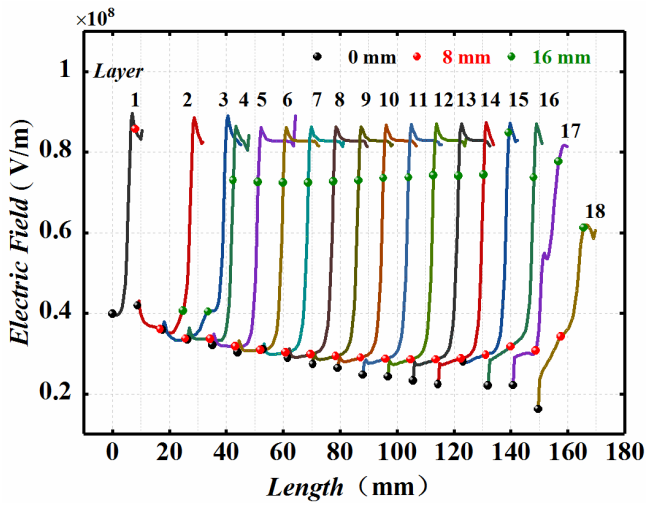

(d)

FIGURE 9. Electric field on the surface of each film layer. (a) electric field on the lower surface of each film layer in Side A. (b) electric field on the upper surface of each film layer in Side A. (c) electric field on the lower surface of each film layer in Side B. (d) electric field on the upper surface of each film layer in Side B.

The electric filed strength on the upper surface of characteristic points in 8mm and 16mm away from the edge of each film layer can be selected to compare the electric field between the inner layers and the outer layers. Fig. 10 (a) shows the total field strength, normal and parallel components of the field at the characteristic points of each layer in Side B. Fig. 10 (b) shows the proportion of parallel and normal components to the total field strength. It indicates that the electric field on the surface of each layer is mainly composed of normal components and the electric field strength on the film surface at the same position of each layer is almost equal in Side B.

Fig. 11 shows the electric field and the proportion at the characteristic points of each layer on the conical surface in Side A. As shown in Fig.11, it can be found that the total field and the parallel component on the film surface in Side A gradually dropped from the inner layers to the outer layers,

while the parallel component of the field increases continuously. Furthermore, the normal component of the electric field on the inner film layers is much larger than the parallel component, and the parallel component of the field is dominant on the outer film layers.

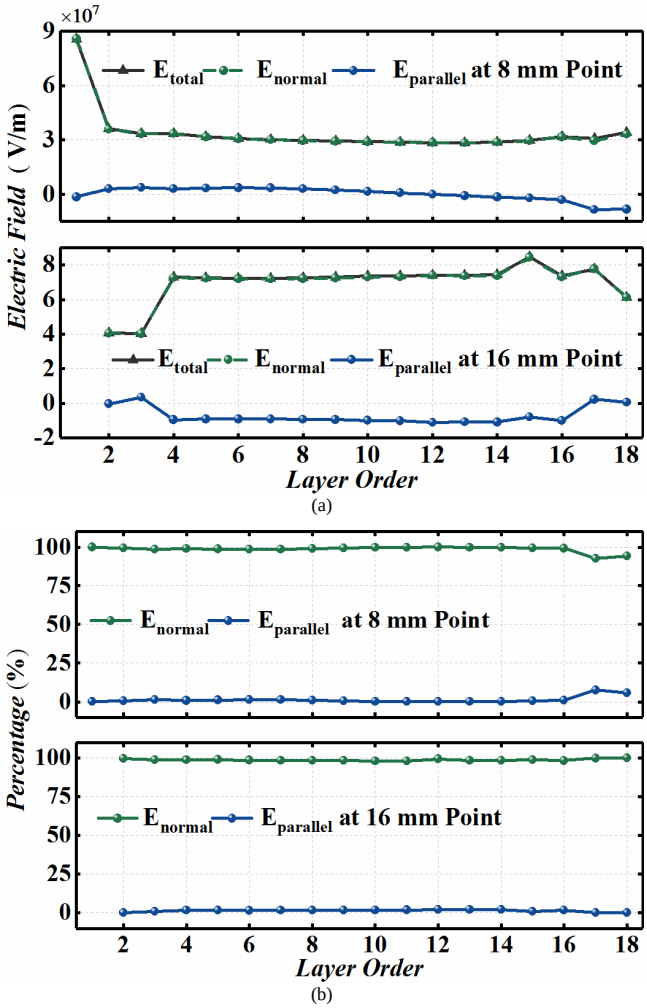

FIGURE 10. **Electric field distribution of each film layer in Side B. (a) electric field. (b) proportion of the component.**

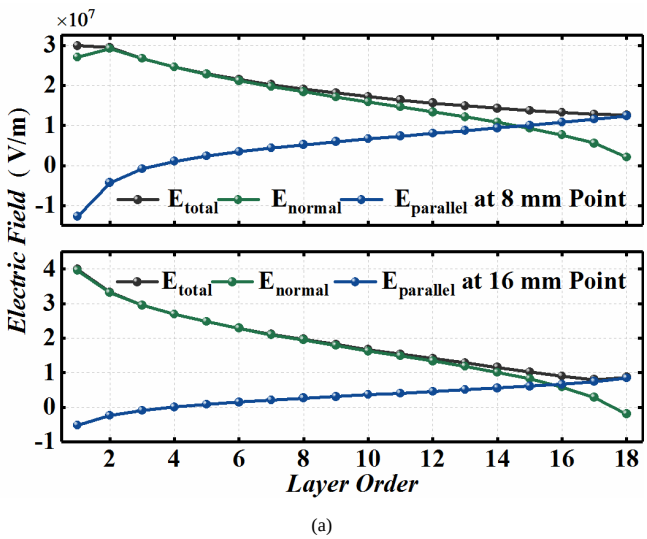

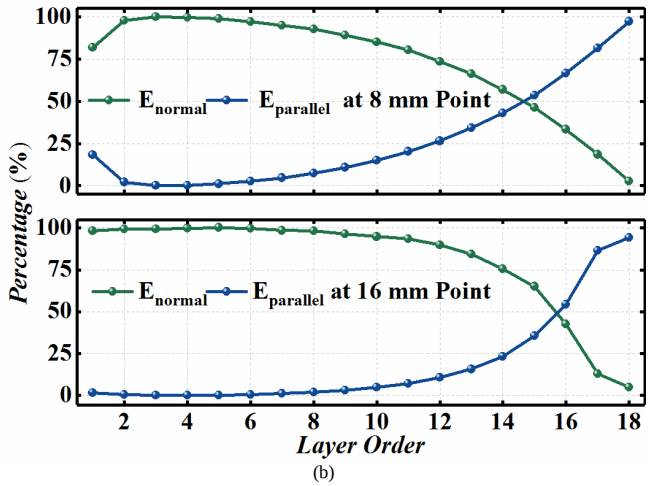

FIGURE 11. **Electric field distribution of each film layer in Side A. (a) electric field. (b) proportion of the component.**

IV. FLASHOVER PROCESS

As shown in Fig. 12, according to the theory of streamer and above analyses, the flashover process of the peaking capacitor can be illustrated with the following four stages.

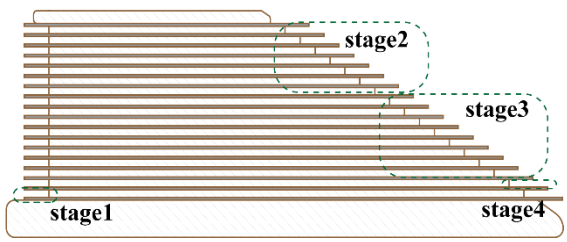

FIGURE 12. **The stages of the flashover process for the peaking capacitor.**

As shown at Stage 1 of Fig. 12, when the high voltage nanosecond pulse is loaded on the peaking capacitor, due to the insulation distance of the lower surface of Layer 1 on the non-conical surface in Side B is relatively short, the flashover would firstly occur in the lower surface of the Layer 1, which leads to the increase of the voltage loaded on the other layers.

The electric field on the outermost layer is approximately parallel to the surface of the film, and the direction of flashover channel is the same as the electric field. In general, the streamers would propagate along the electric field line. Although the total field strength of the inner layers is higher than the outer, the streamer usually developed along the electric line and the flashover should firstly appear on the outer layers. Meanwhile, the results of the circuit simulation show that the earlier the flashover occurs, the smaller the flashover current generates, and the less damage is caused, which is consistent with the damage degree of different layers in the destroyed capacitor. Therefore, as shown at the Stage 2 of Fig. 12, the flashover would firstly occur on the outer layer in Side A, and then streamers might start from the triple point of each film layer and propagate to the edge of the film, resulting in the electrical connection between the

neighboring electrodes. Meanwhile, the voltage applied on the small single coaxial capacitor of other film layer should become much larger.

As shown at the Stage 3 of Fig. 12, the voltage applied on the peaking capacitor rises continuously whilst the voltage on the inner small single coaxial capacitor increases because of the short circuit of the outer small single coaxial capacitor. Although the electric field on the inner conical surface in Side A is mainly composed of the normal component, the total electric field strength is extremely large. The flashover also can originate from the triple point between the inner film and the electrode of each film layer, then develop to the edge of the film, which would lead to the conduction between the adjacent electrodes eventually. Due to the later the flashover occurs, the flashover current is higher than that in the Stage 2, and the damage on the film surface will be more serious, which is consistent with the characteristics of the flashover trace on the film surface of the peaking capacitor as mentioned.

In the Stage 1, the flashover occurs on the Layer 1 in the Side B, so the voltages on upper and lower cylindrical electrodes attached to the Layer 1 are the same. Thus, there is no flashover on Layer 1 in Side A. As shown at the Stage 4, the voltage loaded on the Layer 2 is very high when the flashover appeared on all other layers. The flashover would initiate on both sides of the Layer 2 and meet at the edge of the film, so the upper and lower surfaces of the Layer 2 are severely damaged and the flashover trace are more obvious for the strongest flashover current on both sides of the film layer, so far, resulting in the complete insulation failure of the peaking capacitor.

V. THE FLASHOVER IMAGES OF THE PEAKING CAPACITOR

In order to verify those analyses, the integral images of the gliding spark discharge on the conical surface for the same type of the peaking capacitor without insulation failure is obtained by an optical observation system in stepwise voltage. The charging voltage of the Marx is added from 15 kV, and the flashover images are taken every 5 kV. The insulation environment of the peaking capacitor is full of SF_6 gas with the pressure of 0.8 MPa.

When the charging voltage of the Marx is 15 kV and 20 kV respectively, the output voltage of Marx is about 780 kV and 1010 kV, and the conical surface of the peaking capacitor is shown in Fig. 13, it indicates that there is no sign of the gliding spark discharge.

Fig. 14 shows the flashover images on the conical surface of the peaking capacitor as Marx charged with 25 kV, and the output voltage of Marx is about 1.3 MV. The flashover spots have been found on the outermost layer and adjacent layers in the peaking capacitor, but the spots are relatively dim and amount of the spots is less. It shows that there is no gliding spark discharge with penetration on the film surface and there is also no electric connection between the adjacent layers.

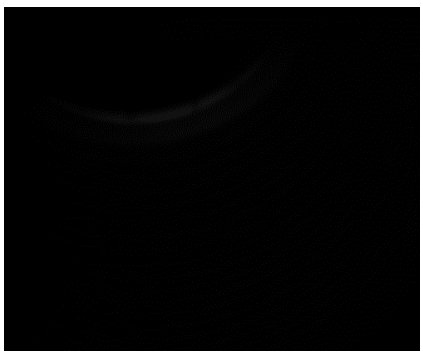

FIGURE 13. The image under the Marx charging voltage of 15 and 20 kV.

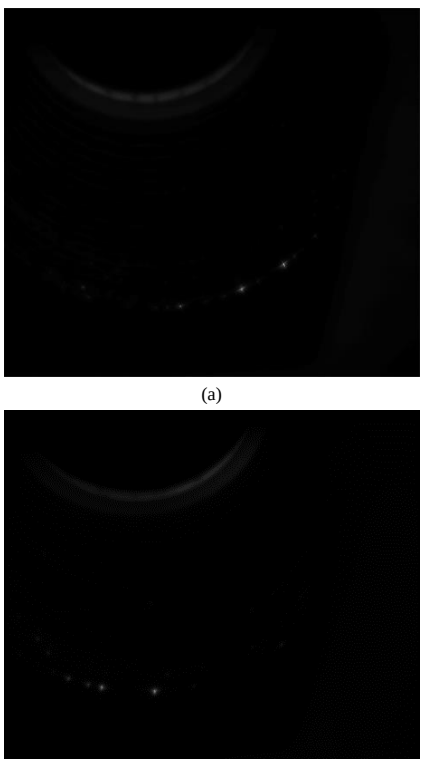

(a)

(b)

FIGURE 14. The images under the Marx charging voltage of 25 kV. (a) type A. (b) type B.

Fig. 15 shows the flashover images on the conical surface of the peaking capacitor as Marx charged with 30 kV, and the output voltage of Marx is about 1.54 MV. There are the larger and brighter spots in Fig. 15 (a), and the gliding spark discharge with penetration occurs in the outer and secondary layers of the peaking capacitor. The number and the brightness of flashover spots decrease from the outer layers to the secondary layers. Fig. 15 (b) shows that the outer layers are covered with many small bright spots, and the gliding spark discharge without penetration arises on the outer layers in Side A. The condition is a critical state in which the gliding flashover with penetration generates on the conical surface in Side A. It could be considered that the

insulation of the peaking capacitor begins to deteriorate from the stage at which the Marx is charged with the voltage of 30 kV, which means that the flashover with penetration would occur under the higher voltage grades.

Fig. 16 shows the flashover images on the conical surface as Marx charging with 35 kV, and the output voltage of Marx is about 1.8 MV. There are much brighter spots and larger scope of the flashover in the outer layer. It is different from critical state that there would be a number of layers with stable gliding spark discharge with penetration on the conical surface.

VI. DISCUSSION

It is apparent from these images on the conical surface of the peaking capacitor that the flashover firstly bursts on the outer layers which are dominant with the parallel component of electric field, and then develops to the inner layers with the increasing voltage. The scope of the flashover also becomes smaller from the outer layers to the inner layers, and these phenomena can also verify the process analyses for the flashover. There is a critical voltage grade of the flashover on the conical surface in Side A, and the flashover discharge with penetration would occur on the film surface between the neighboring layers as the voltage larger than the critical value. Otherwise, there would be only the flashover without penetration between the neighboring layers.

The distribution of electric field on the dielectric surface has an important influence on the surface flashover. The electric field on all the layers are different from each other owing to the special structure of the coaxial and conical peaking capacitor. According to these images and results of the electric field simulation, it can be revealed that although the normal component is prominent on the inner layer, which doesn't lead to the earlier flashover on the inner film layer. Moreover, there are no obvious flashover spots on the non-conical surface dominated with the normal component of electric field. Significantly, this is different from the case that the surface flashover can easily be caused by the intense normal component of electric field on the dielectric surface under the AC, DC and impulse voltage [24]. In the case of nanosecond high voltage pulse, the principal effects of electric field on surface flashover of the peaking capacitor is made by the parallel component rather than the normal component.

For the voltage with a long duration such as AC, DC or lightning impulse, the heat would be easily accumulated due to the intense normal component of the electric field on the surface, so the surface flashover is primarily caused by the thermal ionization. However, it is difficult to form the effective thermal ionization under the nanosecond pulse for the shorter duration, and the flashover can be considered as a process of electron motion. When the direction of the electric field is the same as the channel of the surface flashover, the electron avalanche is easier to generate, so the parallel component of the electric field is more likely to cause the surface flashover under the nanosecond pulse.

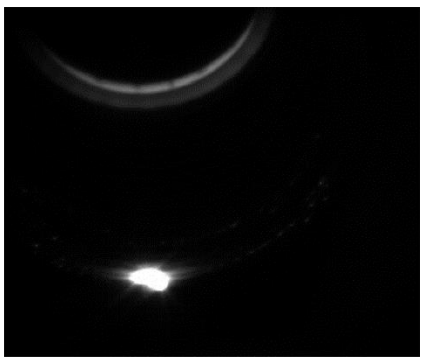

(a)

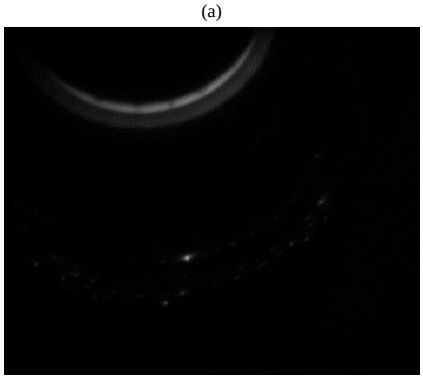

(b)

FIGURE 15. The images under the Marx charging voltage of 30 kV. (a) type A. (b) type B.

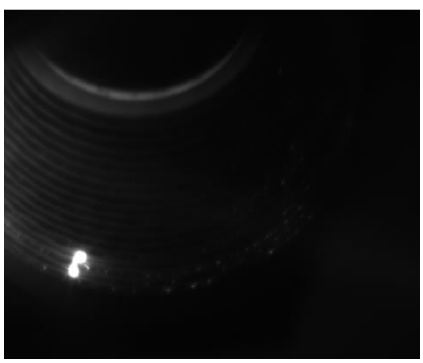

(a)

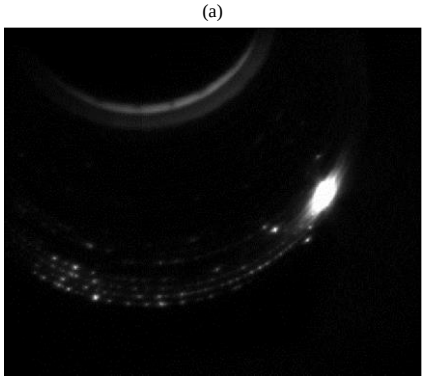

(b)

FIGURE 16. The images under the Marx charging voltage of 35 kV. (a) type A. (b) type B.

VII. CONCLUSION

The process of the flashover for a peaking capacitor in the EMP simulator has been investigated through theoretical analyses and experimental verification in this paper. The characteristics of the damage caused by the flashover and the distribution of the electric filed on the film surface of the peaking capacitor has been introduced. It is argued that the effect of the time sequence on the course of the flashover, and the elementary laws of the occurrence for the flashover on the surface of the peaking capacitor has been found. The main points are as follows:

1) After the insulation failure of the peaking capacitor, the damage on the film surface of the capacitor is gradually more severe from the outer layers to the inner layers.
2) The voltage applied on the rest small single coaxial capacitor will increase when there is the flashover on one single coaxial capacitor. The later the flashover on one single coaxial capacitor occurs, the more serious damage on the surface of the corresponding layer film.
3) The electric field of each layer on the non-conical surface is roughly the same and mainly composed of the normal component. From the outer to inner layers on the conical surface, the total strength and the normal component of the electric field gradually decrease but the parallel component increases. For the conical surface, the normal component of the electric field is much larger than the parallel component on the inner layers, while the parallel component is dominant part of the electric field on the outer layers.
4) For the conical surface of the capacitors, the surface flashover would firstly arise on the outer layers, and then develop to the inner layers as the voltage grade increased.

REFERENCES

[1] A. Qiu, *Application of the pulse power technology*. Xi'an, China: Shaanxi Science and Technology Press, 2016, pp. 276-283.
[2] X. Liu, *High power impulse technique*. Beijing, China: National Defense Industry Press, 2005, pp. 20-23.
[3] I. Smith and H. Aslin, "Pulsed power for EMP simulators," *IEEE Trans. Antennas Propag.* vol. 26, no. 1, pp. 53-59, Jan. 1978.
[4] V. Bailey, V. Carboni, C. Eichenberger, *et al*., "A 6-MV Pulser to Drive Horizontally Polarized EMP Simulators," *IEEE Trans. Plasma Sci.*, vol. 38, pp. 2554-2558, Oct. 2010.
[5] W. Jia, Z. Chen, L. Xie, *et al*., "Simulation analysis for fault states of 2.5 MV electro-magnetic pulse driver with fast rise time," *Journal of Xi'an Jiaotong University*, vol. 46, pp.62-65, Dec. 2012.
[6] Z. Chen, W. Jia, X. He, *et al*., "Double peak phenomenon of applied pulse voltage induced by flashover around parallel-plate electrodes," *High Power Laser and Particle Beams*, vol. 31, no. 7, pp. 1-6, Jul. 2019.
[7] W. Jia, Z. Chen, J. Tang, *et al*., "A 800kV compact peaking capacitor for nanosecond generator," *Review of Scientific Instruments*, 85:094706, Sept. 2014.
[8] Z. Chen *et al*. "A coaxial film capacitor with a novel structure to enhance its flashover performance," *Review of Scientific Instruments*, vol. 85, no. 9, pp. 094706-1-4, Dec. 2019.
[9] X. Zhu, W. Wu, Z. Chen and J. Wei. "Preliminary simulation of radiation field of vertically polarized EMP radiating-wave simulator with peaking capacitor," *Modern Applied Physics*, vol. 11, no.3, pp.44-51, Sept. 2020.
[10] Wilson, *et al*., "Surface flashover of dielectric materials used in pulsed power research," in *16th IEEE Int. Conf. Pulsed Power*, Albuquerque, NM, USA, Jun. 17-22, pp. 2007, pp. 1665-1668.
[11] Y. Cheng, *et al*., "The influence of surface charge accumulation on the vaccum surface flashover characteristic of epoxy resin under nanosecond pulse," in *9th Int. Conf. Properties and Applications of Dielectric Materials*, Harbin, China, Jul. 19-23, 2009, pp. 709-712.
[12] J. Tang, A. Qiu and L. Yang, "Process of Surface Flashover in Vacuum Under Nanosecond Pulse," *IEEE Trans. Plasma Sci.*, vol. 38, no. 1, pp. 53-58, Jan. 2010.
[13] J. Tang *et al*., "The vacuum flashover characteristics of dielectrics under ns pulse," in *IEEE Int. Conf. Solid Dielectrics*, Winchester, UK, Jul. 8-13, 2007, pp. 733-736.
[14] C. Sun *et al*., "Characteristics of nanosecond pulse dielectric surface flashover in high pressure SF6," *IEEE Trans. Dielectr. Electr. Insul.*, vol. 25, no. 4, pp. 1387-1392, Aug. 2018.
[15] Q. Xie, Y. Wang, X. Liu, H. Huang, C. Zhang and T. Shao, "Characteristics of microsecond-pulse surface flashover on epoxy resin surfaces in SF_6," *IEEE Trans. Dielectr. Electr. Insul.*, vol. 23, no. 4, pp. 2328-2336, Aug. 2016.
[16] J.T. Krile, R. Vela and A. Neuber, "Pulsed Dielectric-Surface Flashover in an SF_6 Environment," *IEEE Trans. Plasma Sci.*, vol. 35, no. 5, pp. 1580-1587, Oct. 2007.
[17] M. Zhu, L. Wang, F. Yin, M. Farzaneh, H. Mei and L. Wen, "The Effect of a Vertical Electric Field on the Surface Flashover Characteristics of a Bushing Model," *Energies*, vol. 11, no. 6, pp. 1607-1, Jun. 2018.
[18] L. Liu *et al*., "Investigation on surface electric field distribution features related to insulator flashover in SF6 gas," *IEEE Trans. Plasma Sci*., vol. 26, no. 5, pp. 1588-1595, Oct. 2019.
[19] B.X. Du, R.R. Xu, J. Li, C.L. Han and M.Y. Wang, "Surface Charge and Flashover Voltage of Fluorinated Polypropylene Film under DC and Pulse Voltages," in *IEEE Int. Conf. Dielectrics*, Budapest, Hungary, Jul. 1-5, 2018, pp. 1-4.
[20] B. X. Du *et al*., "Improved charging behaviors and flashover voltage of polypropylene film based on surface molecular structure modification," *Thin Solid Films*, vol. 680, pp. 12-19, Jun. 2019.
[21] Z. Chen *et al*., "Experimental Study of the Breakdown Characteristics of Polypropylene Films Under Nanosecond Voltage Pulses," *IEEE Trans. Plasma Sci.*, vol. 46, no. 11, pp. 4010-4016, Nov. 2018.
[22] Z. Chen, W. Jia, F. Guo, J. Li, W. Wu and S. Ji, "Variation and Saturated Phenomena of Polypropylene Film Flashover Voltage Under Different SF6 Pressures," *IEEE Trans. Plasma Sci*., vol. 47, no. 10, pp. 4553-4559, Oct. 2019.
[23] Z. Chen, W. Jia, F. Guo and S. Ji, "Flashover characteristics of polypropylene films in SF6 using nanosecond pulses," *IEEE Trans. Dielectr. Electr. Insul.*, vol. 27, no. 1, pp. 1-9, Feb. 2020.
[24] Z. Yang, D. Heng, X. Liu, *High voltage insulation technology*. Beijing, China: China Electric Power Press, 2015, pp. 125-126.

Yi Wang was born in Xi'an, China in 1995. He received the B.S. degree in mechanical engineering from Hefei University of Technology, Hefei, China in 2017, the M.S. degree in mechanical engineering from Xi'an Jiaotong University, Xi`an, China in 2020. He is currently a Research Assistant with Northwest Institute of Nuclear Technology, Xi'an, China. His current research interests include the pulse power technology and high voltage surface flashover.

Zhiqiang Chen was born in Hunan, China in 1987. He received the B.S., M.S. and Ph.D. degrees in electrical engineering from Xi`an Jiaotong University, Xi`an, China, in 2009, 2011 and 2020 respectively. He is currently a Research Associate with Northwest Institute of Nuclear Technology. His research interests include the pulse compression technology, and the surface flashover phenomenon in SF6.

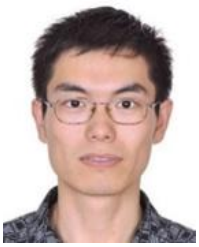

Wei Jia was born in Hebei, China in 1978. He received the B.S. degree in electrical engineering from Xi`an Jiaotong University, Xi`an, China, in 2001, the M.S. degree in nuclear technique and application from Northwest Institute of Nuclear Technology, Xi`an, China, in 2004, and the Ph.D. degree in electrical engineering from Xi`an Jiaotong University, Xi`an, China, in 2019. He is currently a Research Associate with Northwest Institute of Nuclear Technology. His research interests include the development of all kind of Marx generators, the simulation and research of building process of Marx generator, the insulating characteristics of gas and liquid dielectrics, the generation and diagnostic of fast pulse.

Wei Wu was born in Jilin, China in 1976. He received the B.S. degree in biomedical engineering from Jilin University, Jilin, China, in 1999, the M.S. degree in electromagnetic fields and microwave and the Ph.D. degree in nuclear technique and application from Northwest Institute of Nuclear Technology, Xi`an, China, in 2007 and 2020, respectively. He is currently a Senior Engineer with Northwest Institute of Nuclear Technology. His research interests include the simulation of system-generated electromagnetic pulse caused by emitted photoelectron, design of electromagnetic pulse simulator and measurement of pulse electromagnetic field.

Le Cheng was born in Shaanxi, China, in 1995. He received the B.S. and M.S. degrees in electrical engineering from Xi'an Jiaotong University, Xi'an, China, in 2016 and 2019, respectively. He is currently a Research Assistant with Northwest Institute of Nuclear Technology. His current research interests include pulsed power technology, solid-state switch-based nanosecond pulse generators, and plasma applications.

Linshen Xie was born in Fujian, China in 1982. He received the B.S. degree in electrical engineering from Xi`an Jiaotong University, Xi`an, China, in 2005, and the M.S. degree in nuclear technique and application from Northwest Institute of Nuclear Technology, Xi`an, China, in 2008. He is currently a Research Associate with Northwest Institute of Nuclear Technology. His research interests include the development of all kind of Marx generators, the simulation and research of building process of Marx generator, the generation and diagnostic of fast pulse, the generation of electromagnetic pulse environment, measurement and control system of pulse source.

Gang Wu was born in Hubei, China, in June 1982. He received the B.S. and Ph.D. degrees in nuclear engineering and nuclear technology from Tsinghua University, Beijing, China, in 2004 and 2010, respectively. He is currently a Research Associate with Northwest Institute of Nuclear Technology. His research interests include high-altitude electromagnetic pulse environment, effect, and testing methods, pulsed X-ray sources, and system-generated electromagnetic pulse.

Kaisheng Mei was born in Henan, China, in 1994. He received the M.S. degree in electrical engineering from Xi'an Jiaotong University, Xi'an, China, in 2020. He is currently with the Northwest Institute of Nuclear Technology, Xi'an. His research interests include pulsed power technology and high-voltage measurement techniques.